Eur. J. Mech., B/Fluids, **8**, n° 4, 307-326, 1989

Shock-wave annihilation by MHD action in supersonic flows. Two-dimensional steady non-isentropic analysis. "Anti-shock" criterion, and shock-tube simulations for isentropic flows

B. LEBRUN * and J. P. PETIT **

ABSTRACT. — A study of a *shock-wave cancellation* by the action of the *Lorentz force* in *non-viscous supersonic gas* flows is described around slender bodies by a *steady-state two-dimensional analysis.* The hyperbolic flow equations are resolved by the *characteristic method* in the case of a *non-isentropic, plane flow.* These developments lead to an *"anti-shock" criterion.*

Numerical developments in the case of isentropic plane flows in a convergent nozzle allow us to simulate *shock tube* experiments and to confirm the "anti-shock" criterion.

1. Introduction

Shock waves appear in supersonic flows as soon as increases of pressure are induced in the flow [Carriere, 1957], [Courant & Friedrichs, 1948].

The presence of a body involving compression and expansion waves around it is the primary cause of this phenomenon. The shock front involves prompt and abrupt alteration of the flow features:

- increase of pressure, temperature, mass density, entropy,
- decrease of velocity,
- subsonic flow setting up in the case of a straight shock,
- change of velocity direction in the case of oblique shock fronts (with or without subsonic flow setting up).

The Euler equations govern the flow of non-viscous fluids, and for supersonic flows these equations give a hyperbolic system, which we can resolve by the characteristic method. For the two-dimensional steady-state flow the characteristic directions so calculated correspond to the pressure waves, currently called Mach waves.

* Société AS et I, 44, rue R. Salengro, 94126 Fontenay-sous-Bois (France).
** Observatoire de Marseille, impasse du Syphon, 13012 Marseille (France).

0997-7546/89/04 307 20/$ 4.00/

In the convergent regions these Mach waves converge, and if they cross each other in the real space of the fluid there is an accumulation of the pressure perturbations. This produces the shock wave.

It is known that the action of the Lorentz force in conducting fluids permits the modification of the flow features. In the fifties, for instance, many theoretical and experimental developments were made trying to modify the shock-wave system around nose cones. Attempts were made to decrease their velocity and to obtain a better temperature distribution in front of them during the re-entry process [Krank, 1969].

In the sixties, some investigations were made by the Institute of Fluid Mechanic of Marseille (I.M.F.M. France) to study the acceleration of ionized argon flow subjected to a MHD force field [Forestier, 1973], as well as the interaction between an argon flow and an electric field alone [Fontaine, 1973].

Although these studies may have produced understanding of the interaction between a supersonic argon flow and a crossed field $\mathbf{J} \times \mathbf{B}$, they dealt less with the shock wave annihilation.

For the conversion, Sutton [Sutton & Sherman, 1965] has developed a one-dimensional steady state model to describe the behaviour of a supersonic plasma flow in a convergent/divergent nozzle in MHD interaction. He showed that the shock wave rate can be cancelled in a convergent channel if one of the flow features is kept constant by an appropriate force field. On the basis of these developments, [Resler and Sears, 1956] have studied the case of a constant-section channel. They showed that particular conditions on the velocity and the load factor allow the supersonic flow to decelerate to a subsonic one without the establishment of shock conditions.

For the experimental developments, Petit [1983 *a*] carried out shock-wave cancellation and the vanishing of the turbulent wake around a blunt body immersed in shallow salty flow with a Lorentz force field. These investigations showed that the force-field action could accelerate the body. The theoretical analogy between supersonic flows and free-surfade flows allows us to suppose that shock-wave annihilation is possible within gas flows.

A new approach was also developed from an idea suggested by Petit: to cancel shocks around thin bodies, the force fields must keep the parallelism of the characteristic lines issuing from the wall of the body. Indeed, this condition involves the annihilation of the shock waves produced in theory by the self-crossing of these lines.

With these assumptions, the first theoretical developments [Petit & Lebrun, 1986] were made under shock-tube conditions ($p=1$ bar, $T=10{,}000$ K, $M=1{,}6$) in order to show the possibility of experiments with such a device.

Following this, a quasi-one-dimensional steady-state model has been proposed by the authors [Lebrun & Petit, 1989] in the case of a flow around a flat body corresponding to a continuous deviation of the wall, as well as a study about the thermal blockage. These works showed that the Hall effect can advance the shock-wave annihilation and that the parallelism condition involves Sutton's assumptions, *i. e.* $T=\text{Cst}$, $p=\text{cst}$ and $\rho=\text{cst}$ in the interaction region for a perfect gas. These results immediately force the drag to be zero.

In the present work, we investigate the shock-wave annihilation through a two-dimensional analysis, which represents the extention of the first quasi-one-dimensional approach [L & P, 1989]. Our purpose is to study theoretically from the characteristic method the interaction conditions leading to shock-wave cancellation in the case of a perfect gas in non-isentropic interaction for a plane flow. However, the following assumptions are taken to be fulfilled:

- The Hall effect is negligible.
- The magnetic Reynolds number remains weak.

These theoretical developments lead to a general criterion of shock-wave annihilation.

Lastly, a numerical study is done, constituting the first approach of shock-tube simulation. In order to match experimental conditions, the numerical flow parameters used are based on the works of Fontaine [F, 1973] and Forestier [F, 1973]. The optimal conditions brought to the fore by the quasi-one-dimensional analysis [L & P, 1989] correspond to an argon flow at $M=1.6$, $T=9{,}500$ K, $p=1$ bar. The links between such flows and the theoretical assumptions are discussed in Section 5.

2. Establishment of the general equations for a steady-state perfect gas

2.1. The steady-state conservation equations

The equations of the fluid flow describe the conservation of:

- The mass (continuity equation):

(1) $$\nabla . \rho \mathbf{V}=0.$$

- The motion:

(2) $$\mathbf{V}.\nabla \otimes \mathbf{V}+\frac{\nabla p}{\rho}=\frac{\mathbf{J}\times\mathbf{B}}{\rho}.$$

- The energy: this equation takes three equivalent forms:

• The general expression ([S & S, 1965], p. 121):

(3) $$\rho \mathbf{V}.\nabla e+p\nabla.\mathbf{V}=\mathbf{E}^*.\mathbf{J}$$

where $\mathbf{E}^*$ denotes the resultant electric field:

(4) $$\mathbf{E}^*=\mathbf{E}+\mathbf{V}\times\mathbf{B}.$$

• The Bernouilli equation obtained by introducing the enthalpy $h=e+p/\rho$:

(5) $$\rho \mathbf{V}.\nabla\left(h+\frac{\mathbf{V}^2}{2}\right)=\mathbf{J}.\mathbf{E}.$$

• Finally, energy conservation in terms of velocity [L & P, 1989]:

$$a^2 \mathbf{V}.\mathbf{V} - \mathbf{V}.(\mathbf{V}.(\mathbf{V} \otimes \mathbf{V})) = \frac{\mathbf{E}^*.\mathbf{J}}{\rho}(\gamma - 1) - \frac{\mathbf{V}.\mathbf{J} \times \mathbf{B}}{\rho}. \tag{6}$$

2.2. Non isentropic formulation of $\partial\rho/\partial x$

In the following developments, the term $\partial\rho/\partial x$ appears in the continuity equation, and it is advantageous to express it as function of the pressure, in order to obtain a system admitting **V** and p as principal variables. In the case of a non-isentropic flow, we obtain:

$$\frac{\partial\rho}{\partial x} = \left(\frac{\partial\rho}{\partial p}\right)_{s=\text{cst}} \frac{\partial p}{\partial x} + \left(\frac{\partial\rho}{\partial s}\right)_{p=\text{cst}} \frac{ds}{dx}. \tag{7}$$

The Joule effect induces entropy variations which are expressed [S & S, 1965] as:

$$\frac{\partial s}{\partial x} = \frac{\mathbf{J}.\mathbf{E}^*}{\rho \mathrm{VT}}. \tag{8}$$

We must explain the term $(\partial\rho/\partial s)_p$. To do so, we take into account the real gas effects. The state equation is written, according to Norman [1965]:

$$\frac{d\rho}{\rho} = \frac{dp}{p}(1+\mathrm{Z}_p) - \frac{d\mathrm{T}}{\mathrm{T}}(1+\mathrm{Z}_t). \tag{9}$$

The terms Z_p and Z_t mean respectively the compressibility factors at constant pressure and at constant temperature. Then, in the state law (8), expressing ρ and T as functions of the pressure "p" and the entropy "s" yields:

$$\left(\frac{\partial\rho}{\partial s}\right)_p = -\rho \frac{1+\mathrm{Z}_t}{\mathrm{T}} \left(\frac{\partial\mathrm{T}}{\partial s}\right)_p. \tag{10}$$

So, from simple thermodynamic considerations of the entropy expression:

$$\left(\frac{\partial\mathrm{T}}{\partial s}\right)_p = \frac{\mathrm{T}}{\mathrm{C}_p}. \tag{11}$$

Combining the relations (11), (10), (8) and (7) yields finally the density variations:

$$\frac{\partial\rho}{\partial x} = \frac{1}{a^2}\frac{\partial p}{\partial x} - \frac{\mathrm{J}^2(1+\mathrm{Z}_t)}{\sigma \mathrm{VC}_p T}. \tag{12}$$

The coefficients Z_p and Z_t which appear in the above relations are zero for a perfect gas, and then:

$$\frac{\partial\rho}{\partial x} = \frac{1}{a^2}\frac{\partial p}{\partial x} - \frac{\mathrm{J}^2}{\sigma \mathrm{VC}_p \mathrm{T}}. \tag{13}$$

This result, introduced into the continuity equation expressed at the origin of a Lagrangian frame of reference ($u=V$, $v=0$, see *Fig.* 1), provides the required relation (18) taking the Joule effect into account.

When the Joule effect is negligible, the flow can be considered as isentropic and we recover the simple equation relating to this kind of flow:

$$\frac{\partial \rho}{\partial x}=\frac{1}{a^2}\frac{\partial p}{\partial x}. \tag{14}$$

2.3. St. Venant's equation for a MHD interaction flow

The St Venant's equation allows us to determine the sound velocity "a" at any point of the flow submitted to a crossed field. Along a streamline, the energy equation (3) can be written:

$$\frac{\partial}{\partial x}\left(h+\frac{V^2}{2}\right)=\frac{\mathbf{J}.\mathbf{E}^*}{\rho V}+\frac{F_x}{\rho}. \tag{15}$$

For a perfect gas, expressing the enthalpy as function of the sound velocity we obtain along a streamline:

$$\frac{2\,a\,da}{\gamma-1}+V\,dV=\left(\frac{J^2}{\sigma\rho V}+\frac{J_y B}{\rho}\right)dx. \tag{16}$$

When the local velocity, the force-field pattern and the Joule effect are known, this equation allows us to determine the sound velocity, but we can derive the Mach number as well ($M=V/a$):

$$\frac{dM}{M}=\frac{dV}{V}\left(M^2\frac{\gamma-1}{2}+1\right)-\left(\frac{J_y B}{\rho V^2}+\frac{J^2}{\sigma\rho V^3}\right)M^2\frac{\gamma-1}{2}dx. \tag{17}$$

The parameters of the force field are established from the location of the wall electrodes and the geometry of the magnetic field. The velocity can be obtained from the resolution of the hyperbolic-equation system (1) and (2).

3. Characteristic method applied to a plan supersonic flow, in interaction with a crossed force field $J \times B$

This method consists of writing a linear combination of the conservation equations, and then looking for the directions along which the differentials of the variable are total. They are the characteristic directions, which we introduce again into the linear combination in order to obtain the compatibility relations linked with such directions [C & F, 1948]. With the Mach number following from the conservation of the energy, these remain three equations (1) and (2) with three principal unknowns which are the pressure "p", the local velocity V as well as its direction φ.

The conservation equations are written at the origin of a Lagrangian coordinate system:

$$\rho a^2 \left(\frac{\partial u}{\partial x} + \frac{\partial v}{\partial y} \right) + V \frac{\partial p}{\partial x} = \frac{J^2 a^2}{\sigma C_p T} \tag{18}$$

$$u \frac{\partial u}{\partial x} + \frac{1}{\rho} \frac{\partial p}{\partial x} = J_y B = F_x \tag{19}$$

$$u \frac{\partial v}{\partial x} + \frac{1}{\rho} \frac{\partial p}{\partial y} = -J_x B = F_y. \tag{20}$$

The three characteristic directions obtained, depending only on the partial derivatives, are the same as in classical gas dynamics [C, 1957] [C & F, 1948]. We thus obtain along the x-axis:

$$u\,dy - v\,dx = 0 \quad \Rightarrow \quad V\,du + \frac{dp}{\rho} = \frac{J_y B}{\rho} dx \tag{21}$$

which corresponds to the equation (2) in the one-dimensional formulation. For $\mathbf{dy/dx} = \pm \operatorname{tg} \alpha$, the following condition is obtained:

$$\frac{dv}{V} + \frac{dp}{\rho V^2} \frac{dx}{dy} = \left(-\frac{F_x}{\rho V^2} \frac{dy}{dx} + \frac{F_y}{\rho V^2} \right) dx + \frac{J^2}{\sigma \rho V C_p T} \operatorname{tg} \alpha\, dx. \tag{22}$$

We shall do note by η the characteristic direction corresponding to $(+\operatorname{tg}\alpha)$ and ξ the one corresponding to $(-\operatorname{tg}\alpha)$ as shown in Figure 1 [C, 1957].

In the relation (22), the terms taking the force field into account along the two characteristic directions η and ξ can be expressed as:

$$\sin\alpha\, F_x + \cos\alpha\, F_y = F_\eta \sin 2\alpha = F_{\perp\xi} \tag{23}$$

$$\sin\alpha\, F_x - \cos\alpha\, F_Y = F_\xi \sin 2\alpha = F_{\perp\eta}. \tag{24}$$

From Figure 1 we notice that the quantity $(F_\eta \sin 2\alpha)$ represents the intensity of the force perpendicular to the direction ξ. That is the same for $(F_\xi \sin 2\alpha)$ and η. Following this remark, the two projections of the force field are denoted $F_{\perp\eta}$ et $F_{\perp\xi}$. We remark that only the force-field components which do not produce any work along the characteristic lines are taken into account. Actually, the force-field components which appear in these equations are perpendicular to the displacements.

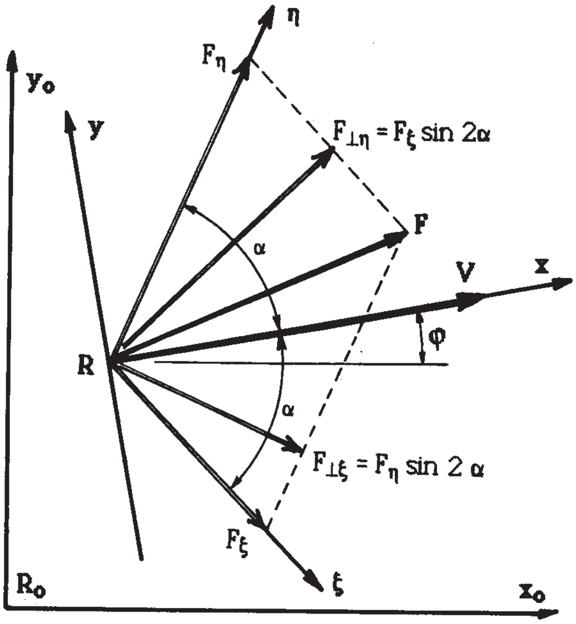

Fig. 1. – Different frame of reference and force field.

Let φ be the angle between the local velocity vector and the x-axis of the frame R_0 associated with the laboratory (*Fig.* 1). Notice that in the coordinate system R associated to the streamlines, we have $du = dV$, and $dv = V.d\varphi$. Furthermore, for a displacement along the direction η, $d\xi$ is zero, so $d. = \partial./\partial\eta\, d\eta$ and along the direction ξ, in the same way, $d\eta = 0$ and $d. = \partial./\partial\xi\, d\xi$. In conclusion, the compatibility conditions along the characteristic directions are as folows:

$$\frac{\sin\alpha\cos\alpha}{\gamma p}\frac{\partial p}{\partial\eta} + \frac{\partial\varphi}{\partial\eta} = -\frac{F_{\perp\eta}}{\rho V^2} + \frac{J^2}{\sigma\rho V C_D T}\sin\alpha = 2\frac{\partial\mu}{\partial\eta} \tag{25}$$

$$\frac{\sin\alpha\cos\alpha}{\gamma p}\frac{\partial p}{\partial\xi} - \frac{\partial\varphi}{\partial\xi} = -\frac{F_{\perp\xi}}{\rho V^2} + \frac{J^2}{\sigma\rho V C_p T}\sin\alpha = 2\frac{\partial\lambda}{\partial\xi} \tag{26}$$

and along the x-axis:

$$dV = -\frac{dp}{\rho V} + \frac{J_y B}{\rho V}dx. \tag{27}$$

The variables λ and μ are called the epicicloidal coordinates as defined by Carrière [1957] for example.

In a free plane flow, for no applied field, the classical solution is indeed recovered. For this case, the right-hand side of the equations (25) and (26) is zero, so that $(\partial\lambda/\partial\eta)$ and $(\partial\mu/\partial\xi)$ are zero for each point of the flow. So λ is constant along $\xi\,(\lambda = \lambda(\eta))$ and also μ is constant along $\eta\,(\mu = \mu(\xi))$.

Now, in the interaction region along these characteristic directions, λ and μ vary as functions of the geometry and the intensity of the force field, and as functions of the Joule effect.

We may always introduce the Busemann number **P** defined as [C, 1957]:

$$d\mathbf{P} = dp\,\frac{\sin\alpha\cos\alpha}{\gamma p}. \tag{29}$$

But this parameter is no longer only a function of α, because the St Venant's equation (18) associated with the relation (22) leads to:

$$d\alpha = d\mathbf{P}\,\frac{\gamma-\cos\alpha}{2\cos^2\alpha} + \left(J_y B - \frac{J^2(\gamma-1)}{2\sigma V\sin^2\alpha}\right)\frac{\operatorname{tg}\alpha}{\rho V^2}\,dx. \tag{30}$$

Without MHD interaction, we thus recover the expression involving integration of **P** as function of α, following the Busemann method [C, 1957] which gives:

$$\mathbf{P} = -\alpha - \sqrt{\frac{\gamma+1}{\gamma-1}}\operatorname{Arctg}\left(\frac{1}{\sqrt{(\gamma+1)/(\gamma-1)}\operatorname{tg}\alpha}\right). \tag{31}$$

In the interaction region and behind it, the Mach number is no longer linked only to the Busemann number **P** and must be calculated by integration of the St Venant's equation along a streamline.

In any case, **P** and φ remain linked with the epicicloidal coordinates through the integration of the relations (25) and (26). At any point of the flow, they can be written:

$$\varphi = \mu - \lambda \tag{32}$$

$$\mathbf{P} = \mu + \lambda. \tag{33}$$

According to the equations (25) and (26), the Joule effect remains negligible if the current density is such that:

$$J \ll \frac{B\sigma C_p T}{V} = J_c. \tag{34}$$

For the numerical simulations performed in Sect. 5, this condition is fulfilled and so the flow can be considered as an isentropic one ($J/J_c \approx 10^{-1}$).

4. "Anti shock" criterion

A slender body embedded in a supersonic flow must induce the convergence and the self-cutting of the characteristic lines issued from the wall, involving the occurrence of a shock wave. However, a force field applied in the range of influence of the bump can balance the effects of local pressure waves induced by the wall and restore the characteristic parallelism far from the wall.

This condition, suggested by Petit, is the basis of the anti-shock criterion. It amounts to considering $\varphi+\alpha$ to be constant in the whole unperturbed flow.

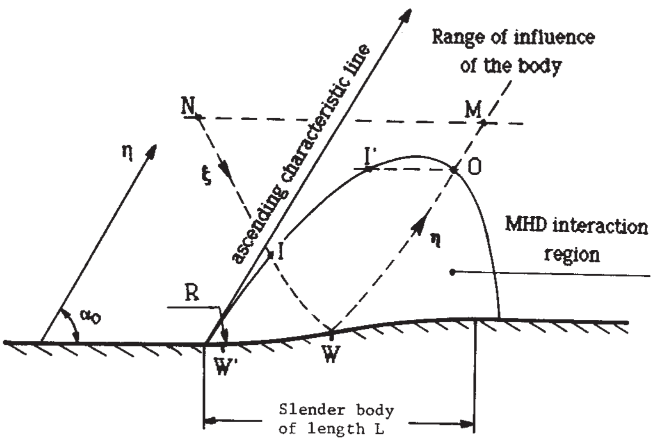

Fig. 2. — Localization of the force field around a slender body.

4.1. General formulation

So consider the following path, described in Figure 2: start from a point N located in the upstream flow of the slender body, and follow the descending characteristic ξ passing through this point. This path enters the perturbed region at the point I. Then it is reflected at the wall at the point W and follows the ascending characteristic η, leaving the perturbed region at the point O and finally arriving at the point M located on the same streamline as N.

We suppose also that the force field is perfectly delimited by a boundary characterized by the points I and O, which splits the unperturbed flow from the perturbed one. In the first approach, it may be possible to consider the force field delimited by the magnetic field geometry. In the case of an evanescent force field, the flow passes imperceptibly from the unperturbed region to the interaction one, without being able to locate the boundary. In that case, the points I and O cannot be defined.

The flow must pass around the body without producing shocks, which involves the parallelism of the characteristic lines in all the unperturbed flow, denoted by ∞. So at the boundary point O:

(35) $$\alpha+\varphi=\mathrm{Cst}$$

and both the flow direction and Busemann number are defined at O using the relations (32) and (33). First, we assume that the descending characteristic ξ enters the interaction region at the point O. That allows us to write:

(36) $$\lambda_\infty=\lambda_M=\lambda_N=\lambda_I=\lambda_O.$$

The epicicloidal coordinate λ takes the following value at the wall point W, along the descending characteristic from I to W:

$$\lambda_W = \lambda_I + \int_I^W \frac{\partial \lambda}{\partial \xi} d\xi = \lambda_I + \Delta\lambda_{IW}. \tag{37}$$

In the same way, we may write, for from W to O along the ascending characteristic η:

$$\mu_O = \mu_W + \int_W^O \frac{\partial \mu}{\partial \eta} d\eta = \mu_W + \Delta\mu_{WO}. \tag{38}$$

Along the slender body the flow direction φ_W is imposed by the wall ($\varphi_W = \mu_W - \lambda_W$) and μ_O can be obtained as a function of the path along the characteristic lines. This yields finally at O:

$$\varphi_O = \varphi_W + \Delta\lambda_{IW} + \Delta\mu_{WO} \tag{39}$$

$$\mathbf{P}_O = \mathbf{P}_\infty - \varphi_\infty + \varphi_W + \Delta\lambda_{IW} + \Delta\mu_{WO}. \tag{40}$$

Now consider the variations of the Mach number along the streamline passing through O. Its behaviour is described from I′ to O by the condition (30), which is written to a first approximation:

$$\alpha_O - \alpha_\infty = (\mathbf{P}_O - \mathbf{P}_\infty)\frac{\gamma - \cos 2\alpha}{2\cos^2\alpha} + \left(\frac{J_y B}{\rho V^2}\operatorname{tg}\alpha + \frac{J^2(\gamma-1)}{\sigma\rho V^3}\right)\Delta X_{I'O} = \varphi_\infty - \varphi_O. \tag{41}$$

The combination of the relations (42), (43), and (44) leads to:

$$\varphi_\infty - \varphi_W = \Delta\lambda_{IW} + \Delta\mu_{WO} - \left(\frac{J_y B}{\rho V^2}\operatorname{tg}\alpha + \frac{J^2(\gamma-1)}{\sigma\rho V^3}\right)\frac{2\cos^2\alpha}{\gamma+1}\Delta X_{I'O}. \tag{42}$$

This relation corresponds to the general "anti-shock" criterion. The force field must satisfy this criterion to be really adapted to the body.

The entire problem of shock-wave cancellation consists of finding a real force field satisfying this criterion. In the case of a non-evanescent force field, it is always possible to modify the shape of the magnetic field to obtain such a force field, as soon as it is confined within the range of influence of the body, as shown in Figure 2.

4.2. Particular formulations of the "anti-shock" criterion

From the general formulation (42), the general criterion does not allow us to determine explicitly either the force field-intensity or its geometry. We must inevitably use numerical simulations. However, under particular assumptions it is possible to obtain simple formulations of the criterion that bring to the fore the slender feature of the force field.

Let us consider a point W′ near the upstream boundary of the range of influence as shown in the figure 2. In this region, it can be admitted that:

$$\Delta\lambda_{NW} \ll \Delta\mu_{WM} \quad \text{and} \quad \Delta X_{\Gamma O} \ll \Delta\mu_{WM} \tag{43}$$

and, taking a force field $\mathbf{F}=\mathbf{J}\times\mathbf{B}$ of orientation θ with respect to the x_0-axis, we obtain, according to the relation (26):

$$F_{\perp\eta} = F\sin(\alpha-\theta). \tag{44}$$

We may define, to first order, the height of the interaction region as:

$$\Delta\eta_{WO} = \frac{h}{\sin\alpha}. \tag{45}$$

We introduce the relations (43), (44) and (45) into the relation (42) to obtain a criterion allowing us to express the height of the interaction region as a function of the wall direction θ, the flow parameters and the crossed fields: Near the wall, sin $(\varphi/y_0)=1/R$, and we obtain:

$$\frac{JBh}{\rho V^2} = 2\frac{\sin\alpha}{\sin(\alpha-\theta)}\left(\varphi_W + \frac{J^2 h}{\sigma\rho VC_p T}\right). \tag{46}$$

It is interesting to develop three particular cases of force-field direction, for the case of isentropic flows.

- F parallel to the x_0-axis $(\theta=0)$

This assumption corresponds to the experimental conditions holding in a symmetrical Faraday's channel in which the electric field is produced by two opposite segmented electrodes, and with a transverse magnetic field sufficiently weak to cmake the Hall effect negligible, this yields:

$$\frac{JBh}{\rho V^2} = 2\varphi_W. \tag{47}$$

The interaction height is directly proportional to the deviation angle of the wall for small deviations.

- F parallel to the ascending characteristic lines $(\theta=\alpha)$

This case corresponds to the developments of the quasi-one-dimensional analysis [L & P, 1989]. It involves the constancy of the flow parameters along the ascending characteristic lines and it introduces the quasi-one-dimensional analysis [L & P, 1989] as a particular case of this two-dimensional approach.

$$\frac{JBh}{\rho V^2} = \infty. \tag{48}$$

Effectively, the interaction height is theoretically boundless in such a case.

- F perpendicular to the ascending characteristic lines ($\theta = \alpha - \pi/2$)

$$\frac{\mathrm{JB}\,h}{\rho\,\mathrm{V}^2} = \frac{2}{\mathrm{M}}\varphi_{\mathrm{W}}. \tag{49}$$

Notice that the minimal height is obtained for this particular force field orientation ($\partial h/\partial\theta = 0$). This result appears to be a logical conclusion because the velocity variations in supersonic flows are produced perpendicularly to these characteristic directions. So such a force-field orientation must act the most efficiently on the flow.

5. Numerical applications

5.1. Location of the theoretical approach with respect to shock-tube experiments

The present theoretical developments are used to simulate experimentations which may be achieved in a shock tube. An ionized argon flow is assumed to pass through a convergent channel. A shock wave must occur in the convergent section: Figure 3 shows the simulation of such a flow. The birth-place of the shock-wave, corresponding to the self-crossing of the characteristic lines, clearly appears.

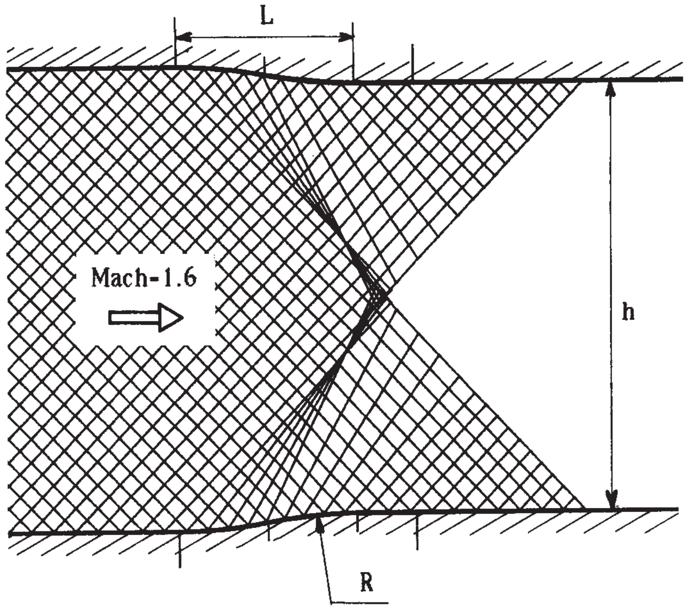

Fig. 3. — Shematic representation of a convergent shock-tube channel.
The merging of the characteristic pattern indicates a shock-wave occurrence.

This representation does not truly have a physical reality, because the shock wave modifies the parameters of the medium in an important way. The convergence of the characteristic lines does not mark the exact location of the shock but only allows us to bring to the fore its occurrence.

So a force field is supposed to accelerate the flow in the convergent part in order to avoid the self crossing of these characteristics lines and allow shock-wave cancellation.

These simulations provide a first account of the phenomena which occur in a shock-tube. Some of the features not taken into account are the non-steady-state feature of the shock tube experiments and the behaviour of the plasma parameters as functions of the temperature and the pressure. Principal properties neglected are the variations of the conductivity σ and the ratio of the specific heats γ, induced by the ionization decreasing or the Joule energy input involving non-thermodynamic equilibrium effects (Te > Tg).

Lastly, the effects of the boundary layer, induced by the viscosity of the plasma, are neglected.

The quasi-one-dimensional analysis [L & P, 1989] enabled us to bring to the fore the optimal conditions to set: this concerns an ionized argon flow at Mach 1.6 at a pressure of 1 Bar:

Mach: 1.6
T: 9,500 K
p: 10^5 Pa.
ρ: 0.050 kg/m^3
V: 2,575 m/s
σ: 2,810 Mhos/m
γ: 1.31.

The Reynolds magnetic number, defined as:

$$R_m = \mu_0 \sigma V L \tag{50}$$

remains smaller than unity (L = 0.04 m) in these conditions, and the flow and the magnetic field can be considered as de-coupled.

Also, a first approach can be made in considering a force field parallel to the wall. The optimal values of the MHD parameters given by the quasi-one-dimensional study [L & P, 1989] were such as the following:

J: 2 10^6 A/m^2.
B: 1 T.
φ: 8° (for a convergent profile of radius R = 0.2 m over a length L/2 = 0.03 m).

With respect to the relation (47), these values lead to an interaction height close to 0.06 m. The force field must then be localized very near the wall and can be defined as slender.

It can be checked that the Joule effect is effectively negligible, because, according to the criterion (34), J is small compared to Jc which is also of order 2×10^7 A/m^2.

In the course of the quasi-one-dimensional study [L & P, 1989], we showed that the Hall effect can advance shock-wave cancellation, in pointing the force field perpendicularly to the ascending characteristic lines. In the present two-dimensional study, this phenomenon is not taken into account in the determination of the force field, although the Hall parameter is of order unity for such interaction conditions.

5.2. Numerical method

We assume the MHD interaction to be isentropic. All the terms taking the Joule effect into account are neglected. The flow can be derived step by step, with respect to the compatibility equations along the characteristic directions, and as a function of the initial and boundary conditions.

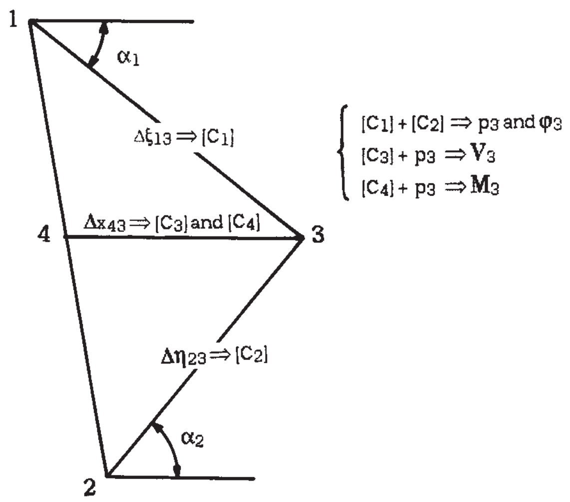

Fig. 4. — Characteristic grid of the numerical scheme.

Let us suppose that, as indicated in Figure 4, at the points 1 and 2 all the MHD parameters are known: M, φ, T, p, F... and the epicycloidal coordinates λ and μ also. The ascending characteristic passing through 2 and the descending characteristic passing through 1 cut in 3, thus defining the displacements $\Delta\eta_{13}$ and $\Delta\xi_{23}$.

The conditions (25) and (26) along the characteristic directions η and ξ are simplified and become:

$$\text{(51)} \qquad [C1] \quad \frac{\sin\alpha\cos\alpha}{\gamma p}\frac{\partial p}{\partial\eta} + \frac{\partial\varphi}{\partial\eta} = -\frac{F_{\perp\eta}}{\rho V^2} = 2\frac{\partial\mu}{\partial\eta}$$

$$\text{(52)} \qquad [C2] \quad \frac{\sin\alpha\cos\alpha}{\gamma p}\frac{\partial p}{\partial\xi} - \frac{\partial\varphi}{\partial\xi} = -\frac{F_{\perp\xi}}{\rho V^2} = 2\frac{\partial\lambda}{\partial\xi}.$$

Thus the fields of λ and μ can be calculated as functions of the force field, for small successive displacements along the characteristic lines η and ξ, which are fixed by the local conditions of the flow. Then the pressure and the flow direction at the point 3 are obtained from discretising the conditions [C1] from 1 to 3 and [C2] from 2 to 3.

Next, along the x direction, from point 4 to point 3, and with respect to the compatibility equation (27) on this direction, the velocity is determined:

$$[\text{C3}] \quad d\mathrm{V} = -\frac{dp}{\rho \mathrm{V}} + \frac{\mathrm{J}_y \mathrm{B}}{\rho \mathrm{V}} dx. \tag{53}$$

Finally, the St Venant's equation (17) allows us to obtain the variations of the Mach number in the x direction:

$$[\text{C4}] \quad \frac{d\mathrm{M}}{\mathrm{M}} = -\frac{dp}{\rho \mathrm{V}^2}\left(1 + \mathrm{M}^2 \frac{\gamma - 1}{2}\right) + \frac{\mathrm{J}_y \mathrm{B}}{\rho \mathrm{V}^2} dx. \tag{54}$$

Thus all the other thermodynamic variables can be determined:

$$\mathrm{T} = \frac{\mathrm{V}^2}{\mathrm{M}^2} \frac{1}{\mathrm{R}\gamma} \tag{55}$$

$$\rho = \frac{p}{\mathrm{RT}} \tag{56}$$

$$a = \sqrt{\gamma \mathrm{RT}}. \tag{57}$$

The resolution of this equation system has been performed with a numerical scheme of second order, which involves an iterative process.

5.3. Force field determination

For a level channel, the force field is obtained from crossing a transverse magnetic field $\mathbf{B} = \mathrm{B}.\mathbf{z}$ and an electric field $\mathbf{E}$ produced by an electric potential between the opposite electrodes, as shown in Figure 5. In the flow, the electrons are subjected to the action of both the applied electric field and the induced electric field $\mathbf{V} \times \mathbf{B}$.

$$\mathbf{E}^* = \mathbf{E} + \mathbf{V} \times \mathbf{B} \quad \Rightarrow \quad \mathbf{J} = \sigma \mathbf{E}^*. \tag{58}$$

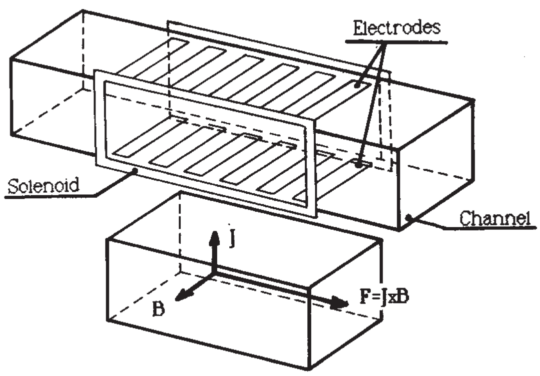

Fig. 5. — Sketch of a linear Faraday convertor.

If the applied field remains constant along the electrodes, and if the acceleration is very strong, the electric field applied to the electrons vanishes very rapidly because of the increasing of the increasing of VB ($\Delta V/V=3$ on a length $\Delta x=0.04$ m [F, 1973]).

To balance the effect of the induced electric field, it would be possible to supply the opposite segmented electrodes with a power device working as a constant-current source rather than a constant voltage one. In these conditions, the voltage between two opposed electrodes is automatically adapted in order to provide a constant current along the whole channel length. That is the accepted solution for the numerical simulations which amounts to considering the electric field **E*** applied to the electrons as deriving from a potential Ψ^*:

$$\Delta\Psi^*=0. \tag{59}$$

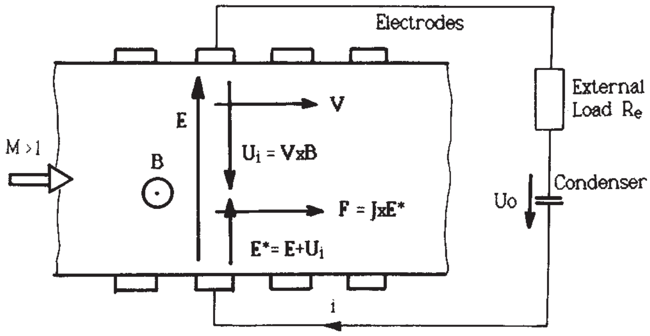

Fig. 6. — Power supply of the electrodes with constant current source.

The flow conditions are such that both the field $\mathbf{V}\times\mathbf{B}$ and the filed **E** are quasi-colinear, giving a situation close to the one-dimensional conditions. Between the electrodes, the power electrical circuit in the steady state is described in Figure 6. Ohm's law corresponding to this circuit is:

$$U_0-VBh=(R_e+R_p)I \tag{60}$$

which gives, on differencing, the sensitivity of intensity to velocity variation:

$$\frac{dI}{dV}=-\frac{Bh}{R_e+R_p}. \tag{61}$$

In order to obtain small variations of the intensity as a function of the velocity, ($\Delta I/\Delta V > -0.1$), according to the relation (69), the power circuit must be equipped with an external load of $1\,\Omega$.

The applied electric field is therefore calculated as a field deriving from a potential, by resolution of the Poisson equation on a square net.

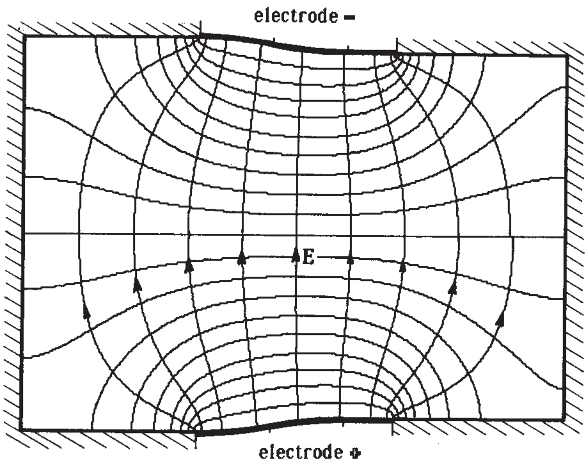

Fig. 7. — Iso-potential and current lines in the convergent channel. Electrodes located on the whole convergent area.

Figure 7 shows the potential lines and the field lines of the electric field used: the electrodes are located along the whole convergent channel.

In the case where the induced field $\mathbf{V} \times \mathbf{B}$ would not be balanced with a constant current source, it would behave as a *regulator* on the flow velocity: actually, in the convergent regions, the flow is slowed down by the wall and E^* would decrease, involving an increasing of the $\mathbf{J} \times \mathbf{B}$ action. On the other hand, in the divergent regions, the velocity increases, which would involve an increasing of $\mathbf{V} \times \mathbf{B}$. Even the case where the acceleration due to the divergent would be such that $\mathbf{V} \times \mathbf{B}$ became greater than $\mathbf{E}$ can be considered. The interaction should pass into a conversion mode, and the flow would be slowed down by the force field.

Thus we can see that the induced field can advance the annihilation of the shock waves, acting like a regulator on the force field, and in fact limiting the pressure variations.

In these numerical simulations, the force field is assumed to be delimited by the geometry of the transverse magnetic field. Two simulation conditions can be distinguished:

– The magnetic field is applied uniformly in the whole channel (*Fig.* 8);

– The geometry of the magnetic field is determined with respect to the "anti-shock" criterion (35) (*Fig.* 9).

5.4. Numerical results

The simulations have been done on a Vax 11/750 and many flow calculations have been performed in the case of a convergent channel.

Figure 3 shows a flow simulation without any force field. The self-cutting of the characteristic lines is brought well to the fore, indicating a shock-wave occurrence. In Figures 8 and 9, the flow is calculated with different force fields, leading to the uncrossing of the characteristic lines.

In these two cases, the force field is about 2×10^6 N/m^3. It is assumed to be achieved with both a magnetic field of one tesla and an electric field having an average value close to 2×10^6 A/m^2.

The radius of curvature of the cylindrical convergent/divergent lengths of the wall is equal to 0.2 m for a height of the shock tube of 0.12 m.

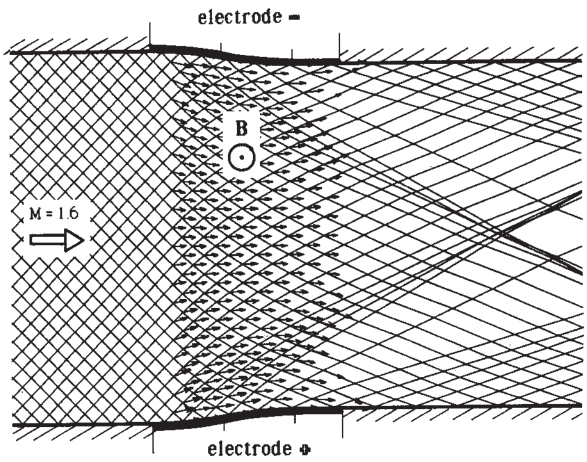

Fig. 8. — Flow simulation with force field applied in the whole channel. $J = 2.2\ 10^6$ A/m^2 on average, B = 1 tesla.

The first calculated flow, shown in Figure 8, is obtained for a force field applied in the whole section of the shock tube and the electric field described in Figure 7. Such a force field leads practically to the uncrossing of the characteristic lines issuing from the convergent part, but the Mach number of the flow is strongly increased: Mach 1.6 at the channel entrance, Mach 2.3 at the exit. In these conditions, it is not easy to deal with the characteristic uncrossing, because the flow is accelerated in a region ahead of the range of influence of the convergent part (median region), which should rather amplify the shock wave. If any other magnetic field is applied along the channel, the crossing of the characteristic lines is only displaced downstream without being annihilated. It shows the necessity of applying the force field only in the range of influence of the convergent part.

Thus this solution has been accepted for the calculation of the flow presented in Figure 9. Furthermore, the magnetic geometry is limited such that the "anti-shock" criterion is checked. In these conditions, the characteristic pattern uncrosses, without any flow acceleration: the force field balances exactly the action of the wall on the fluid. This solution shows the advantage of action in a region near the wall and should allow us to perform analysis for external flows, where the whole body is embedded in the fluid.

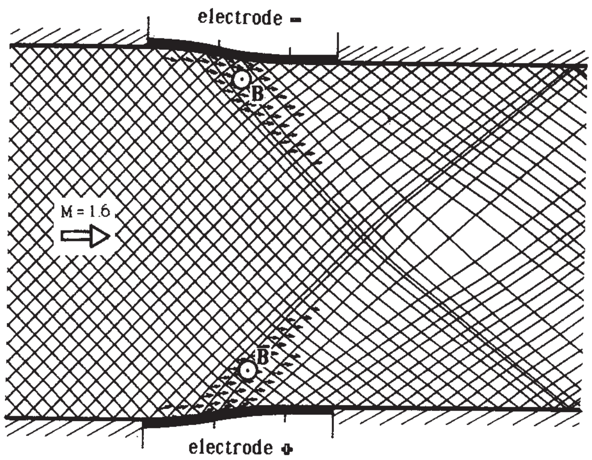

Fig. 9. — Flow simulation with near-parallel force field, checking the "anti-shock" criterion. $J=2\ 10^6\ A/m^2$ on average, B+1 tesla.

6. Conclusion

This two-dimensional steady-state approach for shock-wave annihilation by MHD force-field action allows the ground to be prepare for the study of this phenomenon, following the quasi-one-dimensional study [L & P, 1989].

The "anti-shock" criterion proposed, which is quite simple and seems to be of a very general nature, allows us to determine the geometry of the force field which must be applied in order to annihilate the shock waves induced by a slender body. It shows that the force field must be located near the wall and must balance the pressure variations and the directions variations induced by the wall in the flow.

It seems that a great number of force fields can annihilate the shock waves around same slender body. Thus, from the fundamental point of view, these studies lead to a new class of supersonic flows:

Supersonic flows with flow control in which the shock-waves could be cancelled.

For this two-dimensional study, developed for plane flows, it is relatively easy to modify the geometry of the force field, because the magnetic field is obtained from devices external to the body, the flow being confined in a channel. Moreover, the electric field is practically quasi-one-dimensional, except for the boundary effects. These conditions in the theoretical approach, which are quite simple, present numerous advantages for numerical and experimental developments.

These studies lead to numerical simulations allowing us to simulate shock-tube experiments and to approach the different phenomena which may appear. At the moment, this approach is purely theoretical, but experiments are to be performed in the Laboratoire de Thermodynamique of Rouen's University (LA 230, France) managed by C. Thenard.

Shock-wave annihilation could find applications in channels or ahead of flat or blunt bodies. For this purpose, the future investigations will concern bodies embedded within boundless supersonic flows (external flow) and take the subsonic region into account.

Of course, axi-symmetry flow studies must be developed because, as in MHD conversion using very high magnetic fields, the bodies could be disc-shaped. The numerical simulations will be directed towards finite-element methods which allow us to take into account the boundary layer effect and the subsonic region.

MHD shock-wave annihilation is comparable with MHD propulsion and the most interesting application is the possibility of slender accelerators in sea water or in the atmosphere. Certainly, the Velikov instabilities relating to non-equilibrium ionization of cold gas in the presence of high magnetic fields must occur, but this phenomenon could be avoided by magnetic confinement as suggested by Petit [1983 *b*].

Acknowledgments

We wish to thank here the staff of the numerical centre of the Faculté des Sciences St Charles, of Marseille, where these simulations were performed, and who put their numerical material at our disposal, as well as the French society SOFIMECAL for the financial support that it provides to these research studies.

REFERENCES

CARRIÈRE P., 1957, Méthodes théoriques d'étude des écoulements supersoniques, Publications scientifiques et techniques du ministère de l'air, France.

COURANT R., FRIEDRICHS K. O., 1948, *Supersonic flow and shock waves*, Interscience Publishers, Inc. New York.

FONTAINE B., 1973, *Contribution à l'étude de l'action d'un champ magnétique ou d'un champ électrique transversal sur un courant supersonique d'argon ionisé : cas d'une décharge pure : cas de la conversion MHD*, Thèse N° A 07860, Université de Marseille.

FORESTIER B., 1973, *Étude de l'accélération par les forces de Laplace d'un écoulement supersonique d'argon ionisé*, Thèse N° AO 7861, Université de Marseille.

KRANK S. C., 1969, *Experimental investigation of magnetoaerodynamic flow around blunt bodies*, Ph. D. Eng. Gene., Northwestern University.

LEBRUN B., PETIT J. P., 1989, Shock wave annihilation by MHD action in supersonic flows. Quasi-one-dimensional steady-state analysis and thermal blockage. *Eur. J. Mech. B/Fluids*, **8**, 163-178.

NORMANN W., 1965, One dimensionnal magnetohydrodynamics equations for a non-ideal gas with application to singly ionising argon, *Arn. Eng. Dev. Center-T.R.D.*

PETIT J. P., 1983 *a*, *Is supersonic flight, without shock waves, possible*, Eight Inter. Conf. on MHD Electr. Pow. Gene., Moscow.

PETIT J. P., 1983 *b*, *Cancelletion of the Velikhov instability by magnetic confinment*. Eight Inter. Conf. on MHD Electr. Pow. Gene., Moscow.

PETIT J. P., LEBRUN B., 1986, *Shock wave cancellation in gas by Lorentz Force Action*, Ninth Inter. Conf. on MHD Elec. Pow. Gene., Tsukuba Japan.

RESLER E. L., SEARS W. R., 1956, The prospects for magnetoaerodynamics, *J. Aeron. Sci.*, **25**, 235-246.

SUTTON G. W., SHERMAN A., 1965, *Engineering magnetohydrodynamics*, MacGraw-Hill, New York.

(Manuscript received July 4, 1988,
in revised form: December 12, 1988.)